

Harnessing Adaptive Topology Representations for Zero-Shot Graph Question Answering

Yanbin Wei^{1,2}, Jiangyue Yan¹, Kang Chun, Yang Chen¹, Hua Liu¹, James Kwok², Yu Zhang¹

¹Southern University of Science and Technology ²Hong Kong University of Science and Technology

Abstract

Large Multimodal Models (LMMs) have shown generalized zero-shot capabilities in diverse domain question-answering (QA) tasks, including graph QA that involves complex graph topologies. However, most current approaches use only a single type of graph representation, namely **Topology Representation Form (TRF)**, such as prompt-unified text descriptions or style-fixed visual styles. Those “one-size-fits-all” approaches fail to consider the specific preferences of different models or tasks, often leading to incorrect or overly long responses. To address this, we first analyze the characteristics and weaknesses of existing TRFs, and then design a set of TRFs, denoted by \mathcal{F}_{ZS} , tailored to zero-shot graph QA. We then introduce a new metric, **Graph Response Efficiency (GRE)**, which measures the balance between the performance and the brevity in graph QA. Built on these, we develop the **DynamicTRF** framework, which aims to improve both the accuracy and conciseness of graph QA. To be specific, DynamicTRF first creates a **TRF Preference (TRFP)** dataset that ranks TRFs based on their GRE scores, to probe the question-specific TRF preferences. Then it trains a **TRF router** on the TRFP dataset, to adaptively assign the best TRF from \mathcal{F}_{ZS} for each question during the inference. Extensive experiments across 7 in-domain algorithmic graph QA tasks and 2 out-of-domain downstream tasks show that DynamicTRF significantly enhances the zero-shot graph QA of LMMs in terms of accuracy and brevity simultaneously.

1 Introduction

Large Multimodal Models (LMMs) have served as a universal solution for zero-shot question answering (QA) across a wide range of domains, from commonsense to complex mathematical problem-solving (Kuang et al. 2025). Nevertheless, their zero-shot versatility faces distinctive challenges when answering structured graph problems. First, comprehending the highly structured topology where each node and edge carry explicit relational semantics is difficult for LMMs, because they differ fundamentally from the free-form text or images LMM typically encounter. Besides this structural understanding, another difficulty emerges to perform graph-based execution for specific tasks (e.g., performing Dijkstra’s algorithm (Dijkstra 1959) for shortest-path, Ford–Fulkerson algorithm (Ford and Fulkerson 1956) for maximum-flow) to produce answers for the queries, which demands complex and multi-step computation. Be-

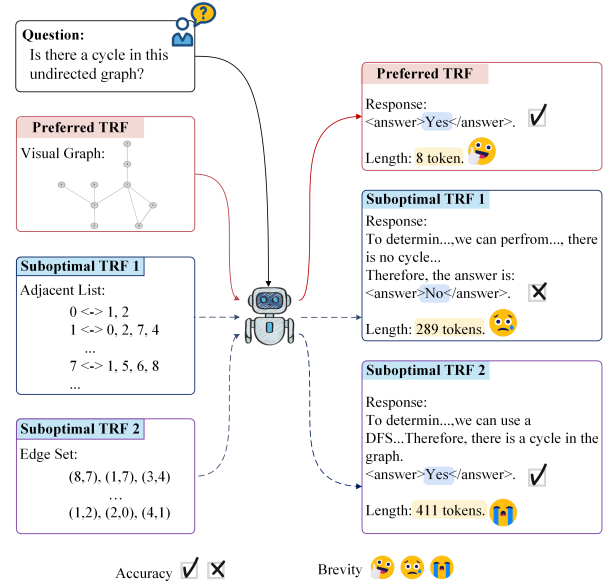


Figure 1: Illustrating the impacts of diverse TRFs on the same question: suboptimal TRFs may lead to wrong answers or unduly lengthy responses compared to a preferred TRF.

sides, in this paper, we focus on zero-shot graph QA, where the model answers questions using only its intrinsic knowledge without task-specific fine-tuning or in-context examples. This setting amplifies the aforementioned challenges, as the LMM has neither prior exposure to the given graph nor the opportunity to learn algorithmic routines on the fly.

Existing works have adopted various topology representation forms (TRFs) to present graph topology to LMMs for understanding. Textual TRFs, as demonstrated in (Ye et al. 2023; Wang et al. 2023; Chen et al. 2024a; Perozzi et al. 2024; Jin et al. 2024), encode graph structures into textual descriptions using diverse prompt templates. Recently, visual TRFs have been introduced for LMMs (Li et al. 2024; Wei et al. 2024b), which depict graph topologies as stylized images. Despite these advancements, existing methods share a common assumption: employing a single type of TRF throughout the QA process, such as unified prompt-based textual descriptions or fixed-style visualizations. This “one-

size-fits-all” approach overlooks critical factors, including model-specific cognitive biases and task-specific representational preferences, resulting in suboptimal QA performance in specific tasks (see experiments in Table 5). Cases in Figure 1 demonstrate the QAs for the same question with diverse TRFs. As can be seen, compared to the preferred TRF, suboptimal TRFs can impede the model’s comprehension of graph topology, resulting in a wrong answer or prolonged response. This raises intriguing research questions: *Can these preferences for TRFs be leveraged? How and to what extent can they enhance the graph QA capabilities of LMMs?*

In this paper, we aim to address these questions through a systematic solution. Specifically, we first categorize and analyze the characteristics of existing representative TRFs. We then design and construct a TRF set \mathcal{F}_{ZS} tailored to zero-shot graph QA, under dedicated design principles. Subsequently, we propose the **DynamicTRF** framework, which operates based on the TRFs within \mathcal{F}_{ZS} and comprises three key components: (1) defining the **Graph Response Efficiency (GRE)** metric, which balances accuracy and computational cost; (2) leveraging a probe dataset to identify TRFs within \mathcal{F}_{ZS} that have optimal GRE for each question, thereby constructing a model-specific **TRF Preference** dataset; (3) training a **TRF Router** on the TRF Preference dataset to dynamically select appropriate TRFs from \mathcal{F}_{ZS} for each question during inference. Note that since the TRFs act at the input stage of LMMs, DynamicTRF does not require access to any information about the model architecture or parameters, and thus can be applied to the state-of-the-art closed-source LMMs. We conduct extensive evaluations across 9 graph QA tasks, encompassing 7 in-domain algorithmic graph QA tasks and 2 out-of-domain downstream tasks. Results show that DynamicTRF enables adaptive question-specific TRF routing, balancing the QA accuracy and response brevity.

Our key contributions are summarized as follows.

- We systematically investigate and discuss the existing fixed TRFs with their characteristics and limitations.
- We propose the GRE metric to quantify the accuracy-brevity trade-off for the graph QA process.
- We propose DynamicTRF, the first framework that integrates LMM graph QA with dynamic TRF routing.
- The side-product TRFP dataset, along with our experiments, offers valuable insights into specific TRFs favored by different task categorizations.
- Comprehensive results show the superior performance of DynamicTRF in zero-shot graph QA across 7 in-domain and 2 out-of-domain downstream tasks.

2 Related Work

LMM-based Graph QA. Graph QA presents unique challenges for LMMs. These challenges stem from the need for structural awareness of graph topology and the ability to select and emulate appropriate algorithms for multi-step reasoning. Existing research in this domain can be broadly categorized into two main approaches: (1) Toolkit-Enhanced System: This category encompasses methods

such as StructGPT (Jiang et al. 2023), Graph-Toolformer (Zhang 2023), and GraphDPR (Li et al. 2024). These systems utilize predefined external toolkits to assist LMMs in graph QA. Although effective within certain domains, this dependence restricts the rigid question types they can handle, rendering them inadequate for out-of-domain tasks. (2) Graph-Aware LMMs: Examples in this category include InstructGLM (Tang et al. 2023), GraphToken (Perozzi et al. 2024), GraphLLM (Chai et al. 2023), and Gcoder (Zhang et al. 2024). These methods enhance LMMs with graph-awareness by modifying their architecture or fine-tuning their parameters, leveraging the internal knowledge of the LMMs for graph QA. Yet the additional training or architectural change breaks the zero-shot premise and makes deployment infeasible on closed-source models that provide only black-box access.

3 Zero-shot TRF Set \mathcal{F}_{ZS}

This section first categorizes and analyzes the existing representative TRFs. It then proposes important principles for designing a Zero-shot TRF Set \mathcal{F}_{ZS} , and constructs an instance of \mathcal{F}_{ZS} following the proposed principles.

3.1 Analyzing TRFs in Graph QA

The TRFs describe the graph topology $G = \{V, E\}$, where V and E denote the set of nodes and edges, respectively. According to the representation types, current TRFs utilized in Graph QA can be categorized into three types: Embedding TRFs, Textual TRFs, and Visual TRFs. In Table 1, we showcase representative TRFs and summarize their characteristics.

TRF	Type	Works	Charac.	Enc.	Train
Embeddings	Embed	GraphLLM(2023), GraphGPT(2023), GraphToken(2024), LLaGA(2024b)	Partial, Informative	Yes	Yes
Visual Graph	Visual	GITA(2024b), VisionGraph(2024)	Full, Intuitive, Explicit	No	No
Edge Set	Textual	GraphWiz(2024a), NLGraph(2023), GPT4Graph(2023), GraphArena(2025), GCoder(2024)	Full, Sequential, Implicit	No	No
Adjacent List	Textual	InstructGLM(2023), GraphText(2023)	Full, Sequential, Implicit	No	No
Adjacent Matrix	Textual	GraphDPR(2024)	Full, Redundant, Implicit	No	No

Table 1: Summary of existing TRFs. ‘Charac.’ indicates the characteristics; ‘Enc.’ and ‘Train’ denote whether the TRF is generated by an external encoder and whether extra training is required, respectively. ‘Embed’ is short for ‘Embedding’.

As the table indicates, Embedding TRFs are generated by

external encoders and typically require alignment training with the embedding space of LMMs (Chai et al. 2023; Tang et al. 2023; Chen et al. 2024b). While the inevitable compression in embeddings leads to the loss of some topological information (Cui et al. 2018), it also allows the learned embedding TRFs to focus on the most informative patterns.

In contrast, both Visual TRFs and Textual TRFs convey the complete topology of a graph, enabling the graph to be uniquely reconstructed from these representations. However, textual TRFs, whether in the form of an Edge Set or an Adjacency List, present complex structures in a flattened, sequential context. This makes the topological information more implicit compared to the intuitive presentation offered by visual graphs (Wei et al. 2024b). Moreover, the Adjacency Matrix often introduces redundant ‘0’ elements for non-existent edges, especially in the case of sparse graphs, making it rarely the primary choice for graph topology representation in existing works. However, the Adjacency Matrix can still be useful in specific scenarios where the explicit representation of connections is advantageous.

3.2 Constructing the \mathcal{F}_{ZS}

Given the variety of available TRFs, we carefully select the most suitable ones to form a dedicated set, denoted as \mathcal{F}_{ZS} , explicitly tailored to zero-shot graph QA scenarios. The selection follows three key principles: (1) *Model-Agnostic*: The generation of TRFs must be decoupled from the LMM parameters, ensuring compatibility with closed-source LMMs. This is crucial as these models often offer superior performance but do not disclose model details. *Consequently, embedding-based TRFs are excluded from \mathcal{F}_{ZS} due to their reliance on embedding spaces, which are inaccessible given most leading models are closed-source.* (2) *Variety*: The TRFs in \mathcal{F}_{ZS} should exhibit diversity to effectively address a wide range of question types. This diversity helps accommodate different types of graphs and QA tasks, utilizing formats like text and images that naturally align with LMM input formats. (3) *Effectiveness*: Each TRF should possess strong individual capabilities, contributing significantly to the overall QA process. This ensures that each component of the set is valuable and enhances the QA performance.

Following these refined principles, we construct an instance of the zero-shot TRF set $\mathcal{F}_{ZS} = \{V_{dot}, V_{neato}, V_{circo}, V_{fdp}, V_{sfdp}, T_{set}, T_{list}, T_{mat}\}$, consisting of the following TRFs:

- Visual TRFs (5 types)**: These TRFs V_{dot} , V_{neato} , V_{circo} , V_{fdp} , and V_{sfdp} are generated based on methods from (Wei et al. 2024b) using different layout algorithms provided by Graphviz (Gansner and North 2000). Specifically, V_{dot} arranges nodes in tree-like hierarchical layers; V_{neato} uses spring model (Fruchterman and Reingold 1991) to minimize edge crossings on canvas; V_{circo} positions nodes in a circular pattern; V_{fdp} offers a fast force-directed layout with optimized computational overhead; and V_{sfdp} provides a scalable force-directed layout for efficiently handling large graphs.
- Textual TRFs (3 types)**: These TRFs T_{set} , T_{list} , and T_{mat} present the graph topology structure via Edge set,

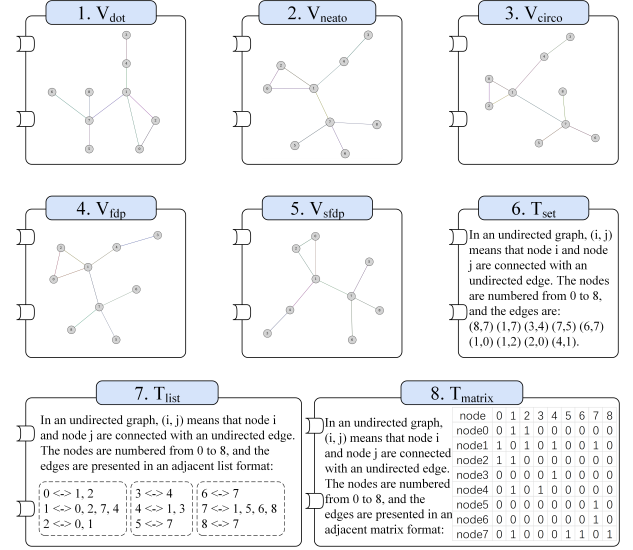


Figure 2: An Illustration of eight candidate TRFs in \mathcal{F}_{ZS} .

Adjacent List, and Adjacent Matrix, respectively. The prompt templates of T_{set} are retrieved from (Wang et al. 2023), and the others are designed by us.

We provide the TRFs generation details in Appendix A.

Figure A4 illustrates the examples of TRFs in \mathcal{F}_{ZS} , all of which are *Model-agnostic* generated before input to LMMs, ensuring their usability with closed-source models. Visual TRFs enable rapid, intuitive perception of topology, while textual TRFs offer slower, analytical understanding, mirroring dual-system cognitive frameworks (Evans 1974; Daniel 2017). Prior works (Wei et al. 2024a; Tang et al. 2025) further show that layouts and prompt templates substantially influence graph QA performance, supporting our emphasis on *Variety*. Section 5.3 empirically validates the *effectiveness* of each TRF across tasks.

4 DynamicTRF

In this section, we present the DynamicTRF framework, which enhances the zero-shot graph QA of LMMs by dynamic TRF routing, on both accuracy and brevity.

4.1 Problem Formulation

LMM-based zero-shot graph QA leverages pretrained LMMs to tackle a wide range of graph problems, without access to or modification of the LMM specifics. This approach facilitates effective generalization across various tasks and unseen graph data, while fully preserving the inherent capabilities of LMMs across the other universal domains.

4.2 Framework Overview

The DynamicTRF framework, shown in Figure 3, establishes a graph QA system with question-specific dynamic TRFs. It consists of two main components: (1) a LMM Reasoner for zero-shot graph QA, and (2) a TRF Router for adaptive TRF selection.

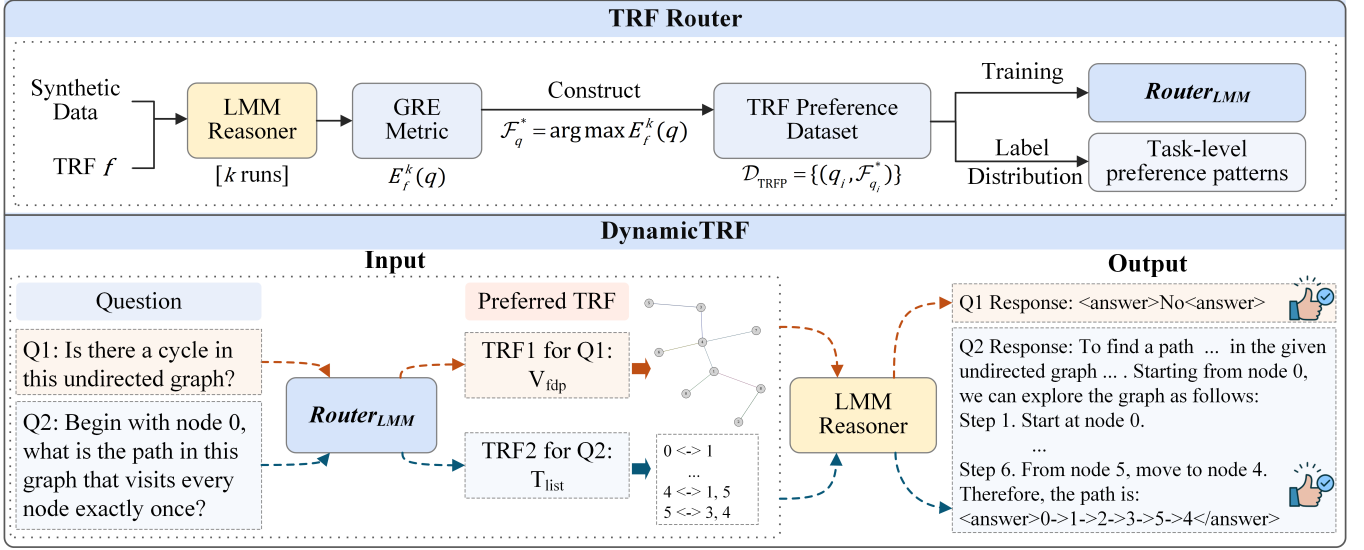


Figure 3: Overview of the DynamicTRF framework, where the TRF Router guides the LMM Reasoner to use the most appropriate TRF based on the question.

DynamicTRF defines a Graph Response Efficiency (GRE) metric to evaluate the trade-off between accuracy and computational cost of TRFs concerning the model and problem context. Using fixed probe data, DynamicTRF identifies the mapping from questions to their optimal TRFs with the highest GRE, creating a TRF Preference dataset to train the TRF Router $Router_{LMM}$.

Then, for any input question q , the TRF Router dynamically assigns the most suitable TRF $f_q \in \mathcal{F}_{ZS}$ and the LMM Reasoner uses f_q as its TRF input to perform zero-shot inference, producing the answer $ans_q^{f_q}$.

4.3 Graph Response Efficiency (GRE)

In this section, we introduce the *Graph Response Efficiency (GRE)* metric, crafted to evaluate the trade-off between accuracy and computational cost among various TRFs.

For a given question q and a TRF $f \in \mathcal{F}_{ZS}$ employed by the LMM Reasoner, the *Graph Response Efficiency* with k random runs is defined as:

$$E_f^k(q) = \frac{100 \times \text{accuracy}_f^k(q)}{(\text{avg.tok}_f^k(q))^\alpha}, \quad (1)$$

where $\text{accuracy}_f^k(q)$ denotes the ratio of correct answers generated by the model in k runs. $\text{avg.tok}_f^k(q)$ represents the average token counts across the k responses from the LMM Reasoner using TRF f . The hyperparameter α regulates the balance between accuracy and token consumption, prioritizing the importance of correct responses relative to the computational cost involved in generating them.

4.4 TRF Preference Dataset

Using the *GRE* metric, we develop the TRF Preference dataset, which explores the mapping from questions to their preferred TRFs. Specifically, we construct

7K QA pairs for in-domain tasks used in Section 5.1, where the graph topology $G = (V, E)$ is randomly generated by Erdős–Rényi (Erdős and Rényi 1960) model (node count $N \in [3, 30]$, edge probability $\in [0.1, 0.7]$) and the response correctness is validated with algorithms. For each question q , its preferred TRFs, denoted as \mathcal{F}_q^* , is determined by:

$$\mathcal{F}_q^* = \arg \max_{f \in \mathcal{F}_{ZS}} E_f^k(q). \quad (2)$$

This equation identifies the set of TRFs \mathcal{F}_q^* that maximize the GRE metric $E_f^k(q)$ for question q . Pairing each question q with its corresponding set of preferred TRFs \mathcal{F}_q^* , we set $k = 10$ and $\alpha = 0.5^1$ to form the TRF Preference dataset, denoted as $\mathcal{D}_{TRFP} = \{(q_i, \mathcal{F}_{q_i}^*)\}$. More details of the TRFP dataset construction method are in Appendix B.

The TRF Preference dataset is a crucial resource for examining the task-level preferences of TRFs. Analyzing the label frequency statistics for specific tasks can reveal the task-level TRF preferences. Table 2 provides the top-3 TRF choices in various tasks of the TRFP dataset, with their frequency to be selected in \mathcal{F}_q^* listed in parentheses.

We can conclude findings from Table 2 by categorizing the 7 tasks into three types: **(1) Perceptual-Intensive Tasks:** Visual TRFs dominate tasks such as Connectivity, Cycle Detection, and Bipartite Graph Matching. These tasks typically require fast and intuitive topology-awareness, which visual representations are well-suited for. **(2) Edge-Weighted Tasks:** Tasks involving edge weights, like Shortest Path and Maximum Flow, prefer textual TRFs. This preference indicates that textual representations are more analytical and suitable for computation-heavy processes. **(3) Ordered Decomposition Tasks:** Hamilton Path and Topological Sorting require ordered decomposition of the graph, and these tasks

¹ α value is user-dependent. We show its impacts in Section 5.3.

Model	TRFs	Conn	Cyc	TS	SP	MF	BGM	HP
GPT-4o	1st	V_{fdp} (92.3%)	V_{sfdp} (85.1%)	T_{set} (58.5%)	T_{set} (19.5%)	T_{list} (21.7%)	V_{dot} (34.2%)	T_{list} (30.4%)
	2nd	V_{neato} (92.1%)	V_{fdp} (12.9%)	T_{list} (36.2%)	V_{neato} (18.7%)	T_{set} (20.8%)	V_{circo} (20.3%)	T_{set} (20.3%)
	3rd	V_{sfdp} (91.7%)	V_{dot} (12.2%)	V_{dot} (23.1%)	T_{list} (17.1%)	T_{mat} (16.7%)	V_{neato} (19.8%)	V_{circo} (18.8%)
Gemini 2.5 Pro	1st	V_{neato} (88.8%)	V_{neato} (97.2%)	T_{set} (41.0%)	T_{list} (48.6%)	T_{mat} (40.0%)	V_{fdp} (24.4%)	T_{list} (42.9%)
	2nd	V_{fdp} (88.2%)	V_{sfdp} (93.0%)	T_{list} (30.3%)	T_{mat} (37.6%)	T_{list} (36.0%)	V_{sfdp} (14.5%)	T_{set} (31.7%)
	3rd	V_{sfdp} (88.2%)	V_{dot} (71.8%)	T_{mat} (15.4%)	T_{set} (26.6%)	T_{set} (14.0%)	V_{neato} (14.5%)	T_{mat} (30.2%)

Table 2: Task-preferred Top-3 TRFs with frequency in TRFP dataset (GPT-4o). ‘Conn’, ‘Cyc’, ‘TS’, ‘SP’, ‘MF’, ‘BGM’, and ‘HP’ denote connectivity, cycle detection, topological sort, shortest path, maximum flow, bipartite graph matching, and Hamilton path. By differing visual or textual TRFs with colors, **the special preference patterns of tasks are explicitly exposed**.

also prefer textual TRFs. This suggests that textual representations facilitate structured and sequential processing. We include the complete ranking of TRF labels with frequency statistics and more analysis in Appendix C.

4.5 TRF Router

The TRF Router constitutes the core decision-making module that dynamically selects a proper TRF $f_q \in \mathcal{F}_{ZS}$ for each question q . Building on our GRE metric $E_f^k(q)$, we formalize the routing strategy through a dual-objective optimization framework that achieves Pareto optimality in accuracy-efficiency tradeoffs.

Pareto Optimal Routing. For each question q , we define 1) Accuracy objective: $\text{Acc}_f^k(q) = \log(100 \times \text{accuracy}_f^k(q))$. 2) Efficiency objective: $\text{Eff}_f^k(q) = -\log(\text{avg.tok}_f^k(q))$. Therefore, according to its definition (equation 1), the logarithm form of the GRE metric $\log(E_f^k(q)) = \text{Acc}_f^k(q) + \alpha \text{Eff}_f^k(q)$. Both objectives become better when they are larger. Taking the logarithm does not change the relative size of numerical values, we have a routing strategy $R \succ R'$ if:

$$\begin{cases} \mathbb{E}_q[\text{Acc}_{f_q^R}^k(q)] \geq \mathbb{E}_q[\text{Acc}_{f_q^{R'}}^k(q)] \\ \mathbb{E}_q[\text{Eff}_{f_q^R}^k(q)] \geq \mathbb{E}_q[\text{Eff}_{f_q^{R'}}^k(q)], \end{cases} \quad (3)$$

with strict inequality in at least one objective, where f_q^R and $f_q^{R'}$ are TRFs selected by R and R' for q , respectively.

Based on this definition, we demonstrate the Pareto optimality of the optimal dynamic routing beyond all the individual TRFs by providing a detailed theorem with proof in Appendix D.

Theorem 1 (GRE-based Dynamic Routing Pareto Optimality). *For any question distribution \mathcal{D}_q and tradeoff parameter $\alpha > 0$, the optimal router R^* satisfying $\forall f \in \mathcal{F}_{ZS}, R^* \succ R_f$, where R^* always select a TRF $f_q^{R^*} \in \mathcal{F}_q^*$, and R_f represents the routing always select f . The strict inequality establishes when f is suboptimal for any $q \in \text{supp}(\mathcal{D}_q)$.*

Router Training. We treat the TRF Router as a classification model (default DeBERTaV3-base) $R_\phi(q) : \mathcal{Q} \mapsto \mathcal{F}_{ZS}$ and train it using the TRFP dataset $\mathcal{D}_{\text{TRFP}} = \{(q_i, F_{q_i}^*)\}$. For each TRF $f \in \mathcal{F}_{ZS}$, we define y_f as an indicator of whether

f is in the true label set F_q^* : $y_f = \mathbb{I}[f \in F_q^*]$ The loss function is then defined as:

$$\mathcal{L}(\phi) = -\mathbb{E}_{(q, F_q^*) \sim \mathcal{D}_{\text{TRFP}}} \left[\sum_{f \in \mathcal{F}_{ZS}} y_f \log p_\phi(y_f | q) + (1 - y_f) \log(1 - p_\phi(y_f | q)) \right],$$

where $p_\phi(y_f | q)$ represents the probability that TRF f is present in the true label set F_q^* . This formulation allows the router to approximate the optimal R^* .

5 Experiment

In this section, we empirically evaluate the proposed DynamicTRF framework.

5.1 Experimental Setup

Datasets. We evaluate DynamicTRF on both seven in-domain graph algorithmic tasks and two out-of-domain downstream application tasks under a zero-shot setting. The in-domain datas are retrieved from GVLQA-BASE benchmark (Wei et al. 2024b), containing tasks including identifying Connectivity (Sedgewick 2001), Cycle (Sedgewick 2001), and computing Topological Sorting (Kahn 1962), Shortest Path (Dijkstra 1959), Maximum Flow (Ford and Fulkerson 1956), Bipartite Graph Matching (Karp, Vazirani, and Vazirani 1990), and Hamilton Path (Gould 2003) (denoted as ‘Conn’, ‘Cyc’, ‘TS’, ‘SP’, ‘MF’, ‘BGM’, and ‘HP’, respectively). For out-of-domain applications, we adopt the ca-GrQC and ca-HepTh (Leskovec, Kleinberg, and Faloutsos 2007) datasets for link prediction (LP), and use the Pol-Blog (Adamic and Glance 2005) and Cora (Yang, Cohen, and Salakhudinov 2016) datasets for the node classification (NC) task. Data and task details are in Appendix E.

Baselines. We evaluate the zero-shot graph QA capabilities of DynamicTRF against the following baselines for in-domain tasks: (1) Vanilla Chain-of-Thought (CoT) (Wei et al. 2022), which uses step-by-step prompts; (2) NLGraph (Wang et al. 2023) that utilizes BAG prompting to conceptualize a graph and algorithmic prompting to specify the algorithm; (3) GraphDPR (Li et al. 2024) employs external tools to generate intermediate descriptions and code with multi-step reasoning; (4) GITA (Wei et al. 2024b) that pairs a vi-

Method	Conn		Cyc		TS		SP		MF		BGM		HP	
	Acc(Tok)	GRE	Acc(Tok)	GRE	Acc(Tok)	GRE	Acc(Tok)	GRE	Acc(Tok)	GRE	Acc(Tok)	GRE	Acc(Tok)	GRE
<i>GPT-4o</i>														
CoT	92.5(273.3)	<u>5.6</u>	52.7(480.6)	2.4	36.6(224.2)	2.4	54.6(566.0)	2.3	25.3(362.9)	1.3	69.5(370.1)	3.6	50.0(124.9)	4.5
NLGraph	92.9(296.6)	5.4	60.2(337.9)	3.3	36.2(<u>202.6</u>)	2.5	59.0(533.7)	2.6	25.6(335.1)	1.4	62.2(<u>356.3</u>)	3.3	57.1(176.5)	4.3
GraphDPR	94.3(412.2)	4.7	68.7(626.4)	2.7	40.2(411.0)	2.0	59.1(496.3)	<u>2.7</u>	31.2(502.7)	<u>1.4</u>	76.5(582.1)	3.2	62.7 (475.8)	2.9
GITA	93.4(285.3)	5.5	64.7(325.7)	<u>3.6</u>	40.9 (256.1)	2.6	56.8(482.1)	2.6	27.4(359.9)	1.4	82.5(392.4)	<u>4.2</u>	54.9(188.8)	4.0
DynamicTRF	96.1(38.8)	15.4	89.3(75.9)	10.3	<u>40.8(176.1)</u>	3.1	68.4 (499.1)	3.1	36.6 (385.2)	1.9	92.0(233.6)	6.0	<u>61.1(76.3)</u>	7.0
<i>Gemini-2.5 Pro</i>														
CoT	97.2(218.7)	6.2	98.6(716.6)	3.7	84.1(1395.9)	2.3	93.6(810.8)	3.3	91.7(1154.9)	2.7	97.1(1076.8)	3.0	96.8(678.1)	3.7
NLGraph	97.3(220.0)	<u>6.5</u>	98.6(629.9)	3.9	84.5(1437.8)	2.2	94.0(847.5)	3.2	92.2(<u>1062.9</u>)	<u>2.8</u>	97.1(1026.4)	<u>3.0</u>	97.1(742.9)	3.6
GraphDPR	<u>98.5</u> (396.6)	4.9	98.9(907.7)	3.3	86.2(1651.4)	2.1	<u>95.5</u> (849.5)	3.3	94.8(1319.6)	2.6	97.8(1187.2)	2.8	<u>97.5</u> (992.9)	3.1
GITA	98.2(238.5)	4.9	<u>99.2</u> (478.9)	4.5	85.5(1398.0)	<u>2.3</u>	94.3(808.2)	<u>3.3</u>	94.2(1155.1)	2.8	<u>99.1</u> (1078.2)	3.0	97.3(679.8)	<u>3.7</u>
DynamicTRF	100(12.9)	27.8	99.3(16.7)	24.3	87.8(1191.2)	2.5	96.3(798.6)	3.4	100(1004.8)	3.2	100(776.0)	3.6	100(254.6)	6.3

Table 3: Zero-shot capabilities on in-domain graph algorithmic tasks. Acc, Tok, and GRE refer to task-average accuracy (%), token consumption, and GRE, respectively.

sual TRF and a textual TRF to collaboratively solve graph algorithmic problems. For monetary cost, we only evaluate all methods with LMMs GPT-4o (OpenAI 2024) and Gemini-2.5 Pro (Google 2025). For each question, we evaluate $k = 3$ times with temperature $\tau = 0.7$. We report the task-average accuracy (noted Acc%) and token cost (noted Tok) across trials, and calculate task-average $GRE = Acc/Tok^\alpha$, $\alpha = 0.5^2$. For out-of-domain tasks, we use the base model, CoT, and GITA as baselines³. Implementation details of all methods are in Appendix F.

5.2 Main Results

Tables 3 and 4 compare the effectiveness (accuracy), efficiency (token consumption), and the trade-off metric GRE of DynamicTRF against baseline methods across seven in-domain and two out-of-domain tasks. DynamicTRF consistently outperforms the baselines by effectively balancing accuracy and efficiency, achieving the highest GRE metric across all models and tasks.

A closer examination of accuracy and token consumption across task types reveals further insights: (1) For perceptual-intensive tasks (Conn, Cyc, BGM), DynamicTRF significantly enhances accuracy while reducing token consumption. These tasks demand rapid and intuitive perception, favoring visual TRFs that excel in both accuracy and token efficiency, thus enabling effective and swift reasoning. (2) In edge-weighted tasks (SP, MF), accuracy is prioritized over token consumption in the trade-off. This is because the routing tends to select TRFs suited for analytical computation, which also incur higher token costs. (3)

²GRE scores averaged on questions are not adopted as metrics since susceptible to outliers.

³Methods like NLGraph and GraphDPR are not applicable due to the absence of definitive algorithms for downstream tasks.

Method	LP		NC	
	Acc(Tok)	GRE	Acc(Tok)	GRE
GPT-4o	71.8(<u>210.5</u>)	5.0	55.7(242.1)	3.6
+CoT	73.2(256.3)	4.6	56.8(291.7)	3.3
+GITA	<u>78.1</u> (224.5)	<u>5.2</u>	60.2(<u>205.5</u>)	<u>4.2</u>
+DynamicTRF	81.4(163.3)	6.5	68.2(126.1)	5.9
Gemini-2.5 Pro	77.2(<u>300.1</u>)	4.3	60.5(330.5)	3.4
+CoT	77.5(330.5)	4.2	60.9(360.8)	3.1
+GITA	<u>80.3</u> (310.2)	<u>4.5</u>	<u>62.8</u> (302.4)	<u>3.7</u>
+DynamicTRF	83.8(225.7)	5.6	72.5(183.6)	5.4

Table 4: Zero-shot capacities on out-of-domain tasks.

For ordered decomposition tasks (TS, HP), the trade-off favors token consumption over accuracy. Specifically, in these tasks, the less prevalent TRFs selected in rare cases are observed to contribute a lot to token savings, revealing the diverse sample-wise demands within these tasks. (4) Despite the out-of-domain nature of downstream applications (LP, NC), the router consistently improves both accuracy and token consumption. This suggests that the advantages of the TRF router can be effectively transferred across domains, enhancing DynamicTRF’s potential as a robust and general solution for improving zero-shot capabilities.

5.3 Ablation Study

Routing Necessity. To elucidate the necessity of the proposed TRF Routing, we present metrics for individual TRFs in Table 5, compared with the proposed TRF Router within the DynamicTRF framework. We also provide performance of ‘Ideal Routing’, where the TRF with the optimal GRE

TRF	Conn		Cyc		TS		SP		MF		BGM		HP	
	Acc(Tok)	GRE	Acc(Tok)	GRE	Acc(Tok)	GRE	Acc(Tok)	GRE	Acc(Tok)	GRE	Acc(Tok)	GRE	Acc(Tok)	GRE
<i>GPT-4o</i>														
V_{dot}	78.5(8.4)	27.1	80.0(8.0)	28.3	12.3(346.0)	0.7	14.5(146.3)	1.2	7.5(410.2)	0.4	91.2(244.3)	5.8	13.3(40.0)	2.1
V_{neato}	95.1(7.7)	34.3	87.1(8.0)	30.8	3.0(30.0)	0.5	20.0(130.1)	1.8	10.8(387.4)	0.5	87.2(280.0)	5.2	11.1(40.0)	1.8
V_{circo}	89.7(8.2)	31.3	70.7(8.0)	25.0	3.0(30.0)	0.5	18.2(153.5)	1.5	8.1(421.3)	0.4	88.2(271.6)	5.3	14.4(40.0)	2.3
V_{fdp}	96.0(8.1)	33.6	60.5(8.0)	21.4	3.0(30.0)	0.5	17.3(150.5)	1.4	8.1(389.2)	0.4	82.9(295.3)	4.8	4.4(74.0)	0.5
V_{sfdp}	94.8(8.1)	33.3	85.1(7.0)	32.2	7.0(120.0)	0.6	25.5(168.7)	2.0	8.1(386.1)	0.4	84.0(302.9)	4.8	12.2(40.0)	1.9
T_{set}	92.5(273.3)	5.6	52.7(480.6)	2.4	36.6(224.2)	2.4	54.6(566.0)	2.3	25.3(362.9)	1.3	69.5(370.1)	3.6	50.0(124.9)	4.5
T_{list}	89.0(218.2)	6.0	53.2(359.7)	2.8	34.2(206.3)	2.4	55.5(518.9)	2.4	24.2(400.7)	1.2	65.8(410.8)	3.2	50.0(107.0)	4.8
T_{mat}	79.9(233.7)	5.2	52.7(417.1)	2.6	6.8(378.1)	0.4	34.5(591.8)	1.4	17.2(402.9)	0.9	60.4(407.3)	3.0	31.1(160.9)	2.5
TRF Router	96.1 (38.8)	15.4	89.3 (75.9)	10.3	41.4 (176.1)	3.1	68.4 (499.1)	3.1	36.6 (385.2)	1.9	92.0 (233.6)	6.0	61.1 (76.3)	7.0
<i>Ideal Routing</i>	100(7.9)	35.6	100(7.1)	37.6	44.5(268.0)	2.7	81.8(223.4)	5.5	53.8(380.0)	2.8	100(181.7)	7.4	76.7(72.2)	9.0

Table 5: Comparison of the DynamicTRF framework with TRF Router versus single TRFs on in-domain tasks. ‘*Ideal Routing*’ means the routing is always to the best TRF. We leave Gemini-2.5 Pro results in Appendix G due to page limit.

is always selected, serving as the upper bound capability of TRF routing. As can be seen, there does not exist any TRF that can dominate the others across tasks. For each task, the top TRFs are highly aligned with the task preferences in the TRFP dataset (Table 2). With the TRF Router, DynamicTRF achieves the highest GRE scores across all tasks beyond all individual TRFs, underscoring its superior performance in balancing accuracy and efficiency. Besides, there is still a gap between the TRF Router and ‘*Ideal Routing*’, highlighting the preserved promising potential of TRF routing.

Sensitivity on α . Table 6 demonstrates the performance effects of varying α values in Eq.(1), where the routers are separately trained on diverse TRFP datasets with updated GRE metrics computed with $\alpha = 0$ and 1. As illustrated, setting a lower $\alpha = 0$ makes GRE dominant by accuracy, thus increasing the accuracy but costing more tokens. Conversely, a higher $\alpha = 1$ value penalizes more on token consumption, resulting in reduced tokens but decreased accuracy.

Metric	α	I.D.	LP	NC	Avg.
<i>GPT-4o</i>					
$\Delta\text{Acc} \uparrow$	0	+0.0	+0.7	+0.5	+0.4
	1	-0.1	-0.4	-0.2	-0.2
$\Delta\text{Tok} \downarrow$	0	+78.8	+45.6	+32.7	+52.4
	1	-2.1	-3.5	-2.2	-2.6
<i>Gemini-2.5 Pro</i>					
$\Delta\text{Acc} \uparrow$	0	+0.7	+1.2	+2.5	+1.5
	1	-19.2	-12.1	-6.9	-12.7
$\Delta\text{Tok} \downarrow$	0	+286.2	+72.9	+83.8	+147.6
	1	-8.5	-4.2	-5.7	-6.1

Table 6: The performance changes with varying the α value from 0.5 to 0/1. ‘I.D.’ means an average on in-domain tasks.

5.4 Router Transferability for LMMs

To evaluate the cross-model generalization of the proposed method, we conducted transfer experiments where the router

Metric	I.D.	LP	NC	Avg.
<i>Transfer Gemini-2.5 Pro’s Router to GPT-4o</i>				
$\Delta\text{Acc} \uparrow$	-0.3(+6.1)	-0.1(+3.2)	-1.4(+6.6)	-0.6(+5.3)
$\Delta\text{Tok} \downarrow$	-35.5(-123.4)	-9.2(-56.4)	-40.1(-119.5)	-28.3(-99.8)
<i>Transfer GPT-4o’s Router to Gemini-2.5 Pro</i>				
$\Delta\text{Acc} \uparrow$	+0.1(+1.9)	+0.5(+4.0)	-0.1(+9.6)	+0.2(+5.2)
$\Delta\text{Tok} \downarrow$	+14.4(-216.2)	+26.9(-47.5)	+3.2(-115.6)	+14.8(-126.4)

Table 7: Performance changes when the LMM Reasoner uses a transferred router from other LMMs in DynamicTRF. Values in parentheses are relative to the best baselines.

trained on one LMM (either GPT-4o or Gemini-2.5 Pro) is directly used by the other without retraining. This setup tests whether TRF preferences learned from one model’s behavior could be effectively leveraged by another. As shown in Table 7, when GPT-4o uses the Gemini-2.5 Pro’s Router, the token count of responses decreases, but the accuracy drops, while using GPT-4o’s router in Gemini-2.5 Pro has the opposite effect. **Anyway, the transferred routers consistently provided benefits** beyond the baselines in terms of both accuracy and brevity. This indicates that the learned TRF preferences show promise in transferring beyond model biases.

6 Conclusion

We propose DynamicTRF, a novel framework to enhance zero-shot graph QA in LMMs. By systematically investigating existing TRF characteristics and proposing the GRE metric, we explicitly observe the diverse preferences on TRFs in graph QAs and highlight the necessity to utilize them. By dynamically assigning proper TRF for queries, DynamicTRF achieves a remarkable balance between accuracy and response brevity without model modification. Extensive experiments across 7 in-domain algorithmic and 2 out-of-domain downstream tasks demonstrate the practicality of DynamicTRF in zero-shot graph QA.

References

- Adamic, L. A.; and Glance, N. 2005. The political blogosphere and the 2004 US election: divided they blog. In *Proceedings of the 3rd international workshop on Link discovery*, 36–43.
- Akoglu, L.; Tong, H.; and Koutra, D. 2015. Graph based anomaly detection and description: a survey. *Data mining and knowledge discovery*, 29(3): 626–688.
- Bellman, R. 1962. Dynamic programming treatment of the travelling salesman problem. *Journal of the ACM (JACM)*, 9(1): 61–63.
- Cao, Q.; Shen, H.; Gao, J.; Wei, B.; and Cheng, X. 2020. Popularity prediction on social platforms with coupled graph neural networks. In *Proceedings of the 13th International Conference on Web Search and Data Mining*, 70–78.
- Chai, Z.; Zhang, T.; Wu, L.; Han, K.; Hu, X.; Huang, X.; and Yang, Y. 2023. Graphllm: Boosting graph reasoning ability of large language model. *arXiv preprint arXiv:2310.05845*.
- Chen, N.; Li, Y.; Tang, J.; and Li, J. 2024a. Graphwiz: An instruction-following language model for graph problems. *arXiv preprint arXiv:2402.16029*.
- Chen, R.; Zhao, T.; Jaiswal, A.; Shah, N.; and Wang, Z. 2024b. LLaGA: Large Language and Graph Assistant. *arXiv preprint arXiv:2402.08170*.
- Cui, P.; Wang, X.; Pei, J.; and Zhu, W. 2018. A survey on network embedding. *IEEE transactions on knowledge and data engineering*, 31(5): 833–852.
- Daniel, K. 2017. *Thinking, fast and slow*.
- Dijkstra, E. W. 1959. A note on two problems in connexion with graphs. *Numerische Mathematik*.
- Edmonds, J.; and Karp, R. M. 1972. Theoretical improvements in algorithmic efficiency for network flow problems. *Journal of the ACM (JACM)*, 19(2): 248–264.
- Erdős, P.; and Rényi, A. 1960. On the evolution of random graphs. *Publ. Math. Inst. Hungar. Acad. Sci.*, 5: 17–61.
- Evans, J. S. B. 1974. Dual processes in reasoning? *Cognition*, 3(2): 141–154.
- Ford, L. R.; and Fulkerson, D. R. 1956. Maximal flow through a network. *Canadian Journal of Mathematics*.
- Fruchterman, T. M.; and Reingold, E. M. 1991. Graph drawing by force-directed placement. *Software: Practice and experience*, 21(11): 1129–1164.
- Gansner, E. R.; and North, S. C. 2000. An open graph visualization system and its applications to software engineering. *Software: practice and experience*, 30(11): 1203–1233.
- Google. 2025. Gemini-2.5 Pro. Technical report.
- Gould, R. J. 2003. Advances on the Hamiltonian problem—a survey. *Graphs and Combinatorics*.
- Guo, J.; Du, L.; Liu, H.; Zhou, M.; He, X.; and Han, S. 2023. Gpt4graph: Can large language models understand graph structured data? an empirical evaluation and benchmarking. *arXiv preprint arXiv:2305.15066*.
- He, X.; Deng, K.; Wang, X.; Li, Y.; Zhang, Y.; and Wang, M. 2020. Lightgcn: Simplifying and powering graph convolution network for recommendation. In *International Conference on Research and Development in Information Retrieval*, 639–648.
- Hopcroft, J.; and Tarjan, R. 1973. Algorithm 447: efficient algorithms for graph manipulation. *Communications of the ACM*, 16(6): 372–378.
- Hopcroft, J. E.; and Karp, R. M. 1973. An $n^{5/2}$ algorithm for maximum matchings in bipartite graphs. *SIAM Journal on computing*, 2(4): 225–231.
- Jiang, J.; Zhou, K.; Dong, Z.; Ye, K.; Zhao, W. X.; and Wen, J.-R. 2023. StructGPT: A General Framework for Large Language Model to Reason over Structured Data. In *Proceedings of the 2023 Conference on Empirical Methods in Natural Language Processing*, 9237–9251.
- Jin, B.; Liu, G.; Han, C.; Jiang, M.; Ji, H.; and Han, J. 2024. Large language models on graphs: A comprehensive survey. *IEEE Transactions on Knowledge and Data Engineering*.
- Kahn, A. B. 1962. Topological sorting of large networks. *Communications of ACM*.
- Karp, R. M.; Vazirani, U. V.; and Vazirani, V. V. 1990. An optimal algorithm for on-line bipartite matching. In *Proceedings of the twenty-second annual ACM symposium on Theory of computing*.
- Kuang, J.; Shen, Y.; Xie, J.; Luo, H.; Xu, Z.; Li, R.; Li, Y.; Cheng, X.; Lin, X.; and Han, Y. 2025. Natural language understanding and inference with mllm in visual question answering: A survey. *ACM Computing Surveys*, 57(8): 1–36.
- Leskovec, J.; Kleinberg, J.; and Faloutsos, C. 2007. Graph evolution: Densification and shrinking diameters. *ACM transactions on Knowledge Discovery from Data (TKDD)*, 1(1): 2–es.
- Li, Y.; Hu, B.; Shi, H.; Wang, W.; Wang, L.; and Zhang, M. 2024. Visiongraph: Leveraging large multimodal models for graph theory problems in visual context. *arXiv preprint arXiv:2405.04950*.
- Newman, M. E.; and Girvan, M. 2004. Finding and evaluating community structure in networks. *Physical review E*, 69(2): 026113.
- OpenAI. 2024. GPT-4o. Technical report.
- Perozzi, B.; Fatemi, B.; Zelle, D.; Tsitsulin, A.; Kazemi, M.; Al-Rfou, R.; and Halcrow, J. 2024. Let your graph do the talking: Encoding structured data for llms. *arXiv preprint arXiv:2402.05862*.
- Sedgewick, R. 2001. *Algorithms in C, part 5: graph algorithms*. Pearson Education.
- Tang, J.; Yang, Y.; Wei, W.; Shi, L.; Su, L.; Cheng, S.; Yin, D.; and Huang, C. 2023. Graphgpt: Graph instruction tuning for large language models. *arXiv preprint arXiv:2310.13023*.
- Tang, J.; Zhang, Q.; Li, Y.; Chen, N.; and Li, J. 2025. Grapharena: Evaluating and exploring large language models on graph computation. In *The Thirteenth International Conference on Learning Representations*.

- Tarjan, R. E. 1975. Efficiency of a good but not linear set union algorithm. *Journal of the ACM (JACM)*, 22(2): 215–225.
- Wang, H.; Feng, S.; He, T.; Tan, Z.; Han, X.; and Tsvetkov, Y. 2023. Can language models solve graph problems in natural language? *Advances in Neural Information Processing Systems*, 36: 30840–30861.
- Wasserman, S.; and Faust, K. 1994. Social network analysis: Methods and applications.
- Wei, J.; Wang, X.; Schuurmans, D.; Bosma, M.; Ichter, B.; Xia, F.; Chi, E. H.; Le, Q. V.; and Zhou, D. 2022. Chain of Thought Prompting Elicits Reasoning in Large Language Models. In *Proceedings of Neural Information Processing Systems*.
- Wei, Y.; Fu, S.; Jiang, W.; Kwok, J. T.; and Zhang, Y. 2024a. Rendering graphs for graph reasoning in multimodal large language models. *arXiv preprint arXiv:2402.02130*, 1.
- Wei, Y.; Fu, S.; Jiang, W.; Zhang, Z.; Zeng, Z.; Wu, Q.; Kwok, J.; and Zhang, Y. 2024b. Gita: Graph to visual and textual integration for vision-language graph reasoning. *Advances in Neural Information Processing Systems*, 37: 44–72.
- Yamanishi, Y.; Araki, M.; Gutteridge, A.; Honda, W.; and Kanehisa, M. 2008. Prediction of drug–target interaction networks from the integration of chemical and genomic spaces. *Bioinformatics*, 24(13): i232–i240.
- Yang, Z.; Cohen, W.; and Salakhudinov, R. 2016. Revisiting semi-supervised learning with graph embeddings. In *International conference on machine learning*, 40–48. PMLR.
- Ye, R.; Zhang, C.; Wang, R.; Xu, S.; and Zhang, Y. 2023. Language is all a graph needs. *arXiv preprint arXiv:2308.07134*.
- Zhang, J. 2023. Graph-toolformer: To empower llms with graph reasoning ability via prompt augmented by chatgpt. *arXiv preprint arXiv:2304.11116*.
- Zhang, Q.; Hong, X.; Tang, J.; Chen, N.; Li, Y.; Li, W.; Tang, J.; and Li, J. 2024. Gcoder: Improving large language model for generalized graph problem solving. *arXiv preprint arXiv:2410.19084*.
- Zhao, J.; Zhuo, L.; Shen, Y.; Qu, M.; Liu, K.; Bronstein, M.; Zhu, Z.; and Tang, J. 2023. Graphtext: Graph reasoning in text space. *arXiv preprint arXiv:2310.01089*.

A A. TRF Generation

In this section, we provide more detailed introductions for the TRFs in \mathcal{F}_{ZS} and their generation approaches. As introduced, \mathcal{F}_{ZS} contains 8 types of dedicated TRFs, where V_{dot} , V_{neato} , V_{circo} , V_{fdp} and V_{sfdp} are visual TRFs, and T_{set} , T_{list} , and T_{mat} are textual TRFs.

More Details for Visual TRFs Generation These visual TRFs are generated by leveraging diverse layout algorithms to compute graph layouts displayed on the canvas, specifically V_{dot} , V_{neato} , V_{circo} , V_{fdp} , and V_{sfdp} . Their generation follows the methodologies outlined in (Wei et al. 2024b) and (Wei et al. 2024a), using the graph visualization tool Graphviz (Gansner and North 2000). To ensure style consistency without unnecessary disturbances, we only vary the layout algorithms while fixing other configurations (white background, circular node shape (except for barpartite graph matching, we use rectangular/circular shape to distinguish the hosts/tasks), default edge thickness) in Graphviz during generation. Specifically, the five visual TRFs, each utilizing a distinct layout algorithm, are introduced as follows:

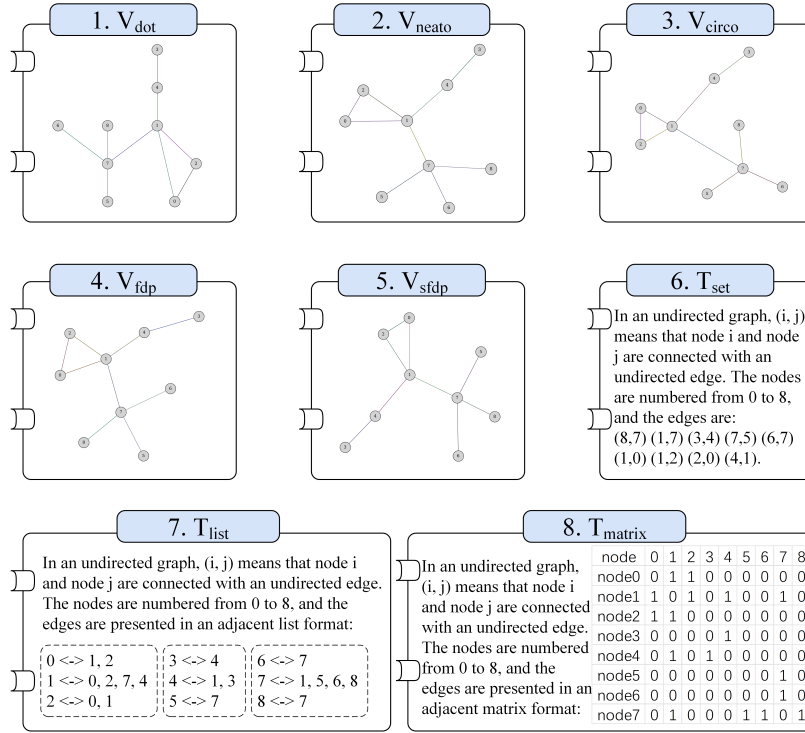


Figure A4: An Illustration of eight candidate TRFs in \mathcal{F}_{ZS} .

- V_{dot} : This visual TRF adopts a hierarchical layout algorithm, which minimizes edge crossings and maintains edge directions (either top-to-bottom or left-to-right). It is particularly effective for representing organizational structures or flowcharts as a visual topology.
- V_{neato} : As a visual TRF, it employs a spring model (Fruchterman and Reingold 1991) layout algorithm. By simulating edges as springs and nodes as mutually repelling entities, it generates an optimal arrangement through force simulation, making it well-suited for visualizing undirected graphs and network relationships.
- V_{circo} : This visual TRF uses a circular layout algorithm that places nodes in a ring structure to reduce edge crossings. It excels at highlighting cyclic topologies, such as those in electronic circuits or advanced abstract syntax trees.
- V_{fdp} : The visual TRF also relies on the spring model but with an optimized algorithm for large graphs. While prioritizing speed, it may sacrifice some node distribution uniformity compared to neato, balancing efficiency and visual clarity for larger topologies.
- V_{sfdp} : This visual TRF incorporates a multi-level force-directed algorithm to extend the fdp layout algorithm to even larger-scale graphs. It maintains force-directed layout characteristics while handling thousands of nodes efficiently, making it ideal for visualizing large topological structures.

To align with the scope of our paper, we do not delve further into additional algorithmic details of these layout methods. For comprehensive implementation specifics of each layout algorithm, readers are referred to the Graphviz technical paper (Gansner and North 2000) and its corresponding Python package documentation. Notably, we have integrated a dedicated interface within

our codebase to facilitate the generation of these visual TRFs, and we recommend that users utilize this interface for direct invocation.

More Details for Textual TRFs Generation The textual T_{set} , T_{list} , and T_{mat} present the graph topology structure via Edge set, Adjacent List, and Adjacent Matrix, respectively. Their prompt templates are detailed in Table A8 to A10. For T_{set} , the prompts are derived from (Wang et al. 2023), while the prompts for T_{list} and T_{mat} are designed and polished by ourselves. To be specific, we introduce these textual TRFs as follows:

- T_{set} : This textual TRF represents graph topology through an unordered collection of edge tuples, where each tuple explicitly denotes a connection between two nodes (e.g., (u, v) for an edge from node u to node v). By omitting redundant structural framing, it achieves high information density, storing all edge relationships in a compact format. This characteristic makes it particularly efficient for tasks requiring quick enumeration of all connections, such as edge existence checks or basic subgraph extraction. However, its unordered nature may complicate reasoning about node neighborhoods or hierarchical relationships, as no implicit grouping of edges by source node is provided.
- T_{list} : Structured as a node-centric inventory, this textual TRF organizes edges by their source nodes, listing all adjacent target nodes for each node in a sequentially ordered format (sorted by node labels). This design strengthens the visibility of neighbor relationships, as all connections originating from a specific node are grouped together, facilitating tasks like neighbor counting, path traversal, or community detection. The sorted arrangement of nodes and edges (by label) further enhances readability, enabling systematic scanning of topological patterns. Compared to T_{set} , it introduces moderate structural overhead but significantly improves accessibility to node-specific relationship information.
- T_{mat} : This textual TRF encodes graph topology as a tabular matrix where rows and columns correspond to nodes, and cell values indicate edge presence (e.g., 1 for an existing edge, 0 for absence). While the inclusion of 0 values for non-edges introduces redundancy, especially in sparse graphs, where most cells are 0, it offers exceptional intuitiveness for visualizing global connectivity patterns. The matrix structure allows for immediate identification of symmetric relationships (via diagonal symmetry) and dense subgraphs (via contiguous blocks of 1s), making it well-suited for tasks like bipartite graph analysis or adjacency pattern recognition. Despite its lower information density, the grid-based format aligns with human cognitive patterns for spatial relationship processing, reducing the cognitive load for certain types of topological reasoning.

Tasks	Template
Connectivity/ Cycle/ Hamilton Path	In an undirected graph, (i, j) means that node i and node j are connected with an undirected edge. The nodes are numbered from $[P]$ to $[P]$, and the edges are: $([P], [P])$, $([P], [P])$...
Topological Sort	In a directed graph with $[P]$ nodes numbered from $[P]$ to $[P]$: node $[P]$ should be visited before node $[P]$ node $[P]$ should be visited before node $[P]$...
Shortest Path	In an undirected graph, the nodes are numbered from $[P]$ to $[P]$, and the edges are: an edge between node $[P]$ and node $[P]$ with weight $[P]$, an edge between node $[P]$ and node $[P]$ with weight $[P]$, ...
Maximum Flow	In a directed graph, the nodes are numbered from $[P]$ to $[P]$, and the edges are: an edge from node $[P]$ to node $[P]$ with capacity $[P]$, an edge from node $[P]$ to node $[P]$ with capacity $[P]$, ...
Bipartite Graph Matching	There are $[P]$ hosts numbered from $[P]$ to $[P]$, and $[P]$ tasks numbered from $[P]$ to $[P]$. Each host has a set of tasks that it is interested in: Host $[P]$ is interested in task $[P]$. Host $[P]$ is interested in task $[P]$
Link Predict/ Node Classify	In an undirected graph, (i, j) means that node i and node j are connected with an undirected edge. The nodes are numbered from $[P]$ to $[P]$, and the edges are: $([P], [P])$, $([P], [P])$... The node attributes are: Node $[P]$, Attribute $[P]$ Node $[P]$, Attribute $[P]$...

Table A8: Prompt templates of T_{set} , where $[P]$ s are placeholders that will be substituted for specific graph topology.

Tasks	Template
Connectivity/ Cycle/ Hamilton Path	<p>In an undirected graph, (i,j) means that node i and node j are connected with an undirected edge. The nodes are numbered from [P] to [P], and the edges are presented in an adjacent list format:</p> <p>[P] <-> [P], [P], [P],...</p> <p>[P] <-> [P], [P], [P],...</p> <p>...</p>
Topological Sort	<p>In a directed graph with [P] nodes numbered from [P] to [P]:</p> <p>node [P] should be visited before node [P], [P], [P],...</p> <p>node [P] should be visited before node [P], [P], [P],...</p> <p>...</p>
Shortest Path	<p>In an undirected graph, the nodes are numbered from [P] to [P], and the edges are presented in an adjacent list format:</p> <p>node [P] is connected to: node [P] with distance: [P], node [P] with distance: [P],...</p> <p>node [P] is connected to: node [P] with distance: [P], node [P] with distance: [P],...</p> <p>...</p>
Maximum Flow	<p>In a directed graph, the nodes are numbered from [P] to [P], and the edges are presented in an adjacent list format:</p> <p>node [P] is connected to: node [P] with capacity: [P], node [P] with capacity: [P],...</p> <p>node [P] is connected to: node [P] with capacity: [P], node [P] with capacity: [P],...</p> <p>...</p>
Bipartite Graph Matching	<p>There are [P] hosts numbered from [P] to [P], and [P] tasks numbered from [P] to [P]. Each host has a set of tasks that it is interested in:</p> <p>Host [P] is interested in tasks [P], [P], [P],....</p> <p>Host [P] is interested in task [P], [P], [P],....</p> <p>...</p>
Link Predict/ Node Classify	<p>In an undirected graph, (i,j) means that node i and node j are connected with an undirected edge. The nodes are numbered from [P] to [P], and the edges are presented in an adjacent list format:</p> <p>[P] <-> [P], [P], [P],...</p> <p>[P] <-> [P], [P], [P],...</p> <p>...</p> <p>The node attributes are:</p> <p>Node [P], Attribute [P]</p> <p>Node [P], Attribute [P]</p> <p>...</p>

Table A9: Prompt templates of T_{list} , where [P]s are placeholders that will be substituted for specific graph topology.

Tasks	Template
Connectivity/ Cycle/ Hamilton Path	<p>In an undirected graph, (i,j) means that node i and node j are connected with an undirected edge. The nodes are numbered from [P] to [P], and the edges are represented in an adjacent matrix format</p> <pre> : node0 1 2... node0 [P] [P] [P],... node1 [P] [P] [P],... node2 [P] [P] [P],... ...</pre>
Topological Sort	<p>In a directed graph with [P] nodes numbered from [P] to [P], the edges are represented in an adjacent matrix format</p> <pre> : node0 1 2... node0 [P] [P] [P],... node1 [P] [P] [P],... node2 [P] [P] [P],... ...</pre>
Shortest Path/ Maximum Flow	<p>In an undirected graph, the nodes are numbered from [P] to [P], and the edges are represented in an adjacent matrix format with weights</p> <pre> : node0 1 2... node0 [P] [P] [P],... node1 [P] [P] [P],... node2 [P] [P] [P],... ...</pre>
Bipartite Graph Matching	<p>There are [P] hosts numbered from [P] to [P], and [P] tasks numbered from [P] to [P]. Each host has a set of tasks that it is interested in</p> <pre> : Task0 1 2... Host0 [P] [P] [P],... Host1 [P] [P] [P],... Host2 [P] [P] [P],... ...</pre>
Link Predict/ Node Classify	<p>In an undirected graph, (i,j) means that node i and node j are connected with an undirected edge. The nodes are numbered from [P] to [P], and the edges are represented in an adjacent matrix format</p> <pre> : node0 1 2... node0 [P] [P] [P],... node1 [P] [P] [P],... node2 [P] [P] [P],... ...</pre> <p>The node attributes are:</p> <pre> Node [P], Attribute [P] Node [P], Attribute [P] ...</pre>

Table A10: Prompt templates of T_{mat} , where [P]s are placeholders that will be substituted for specific graph topology.

B. TRFP Dataset Construction

The TRFP dataset is designed to investigate query-specific preferences among TRFs within \mathcal{F}_{ZS} . To begin with, we generate 1K samples of QA for each task in $\{\text{Conn}, \text{Cyc}, \text{TP}, \text{SP}, \text{MF}, \text{BGM}, \text{HP}\}$, where the graph topologies are randomly generated by the Erdős–Rényi (Erdős and Rényi 1960) model (node count $N \in [3, 30]$, edge probability $\in [0.1, 0.7]$). For SP and MF, the edge weights are randomly assigned $\in \{1, 2, \dots, 10\}$. Graphs that fail to meet task-specific validity criteria are regenerated (We make sure there exists at least a valid answer), ensuring we obtain 7K valid samples (1K per task).

Then, for each question, we evaluate every TRF in \mathcal{F}_{ZS} by running k independent trials to compute the corresponding GRE metric. TRFs are ranked for each question based on their GRE scores in descending order; in cases of tied GRE scores, the tied TRFs are treated as multi-label preferences. By pairing each question with its most preferred TRFs (those with the highest GRE scores), we construct the TRF Preference dataset, denoted as $\mathcal{D}_{\text{TRFP}} = \{(q_i, \mathcal{F}_{q_i}^*)\}$.

To validate response correctness, we use dedicated algorithms for each task:

- Connectivity (Conn) identification answers are judged using the Union-Find algorithm (Tarjan 1975).
- Cycle detection (Cyc) results are verified via Depth-First Search (DFS) (Hopcroft and Tarjan 1973).
- Topological sorting (TS) answers are checked by verifying edge direction constraints in the sequence (Kahn 1962).
- Shortest path (SP) results are validated using Dijkstra’s algorithm (Dijkstra 1959).
- Maximum flow (MF) answers are judged via the Edmonds-Karp algorithm (Edmonds and Karp 1972).
- Bipartite graph matching (BGM) results are verified using the Hopcroft-Karp algorithm (Hopcroft and Karp 1973).
- Hamiltonian path (HP) answers are checked using a backtracking-based approach (Bellman 1962).

The construction of $\mathcal{D}_{\text{TRFP}}$ is contextualized by both the target LMM and the specific definition of the GRE metric. Consequently, distinct LMMs require unique instantiations of the TRFP dataset, while adjustments to the α parameter, which modulates the trade-off between accuracy and brevity in necessitate corresponding updates to $\mathcal{D}_{\text{TRFP}}$ to reflect the shifted weightings in the metric.

C. Label Distributions in TRFP datasets

In this section, we present the complete label distributions of TRFP datasets for both GPT-4o Pro (Table A11). According to this table, we have additional findings beyond those mentioned in the main body of the paper:

- 1) When comparing GPT-4o and Gemini-2.5 Pro, they exhibit highly consistent task-specific TRF rankings, indicating the task-specific TRF preferences can go beyond model biases.
- 2) Specifically, for Conn and Cyc, the suboptimal textual TRFs ($T_{list}, T_{mat}, T_{set}$) also have a consistent inner priority across both models, with $T_{list} > T_{mat} > T_{set}$, highlighting the relative priority of textual TRFs in expressing topological connectivity effectively.
- 3) In the case of GPT-4o, even in tasks where other textual TRFs like T_{list} and T_{set} are preferred, T_{mat} may be suboptimal, indicating a model-specific misalignment with this TRF form. However, this discrepancy is not observed in Gemini-2.5 Pro, suggesting that when someone intends to use T_{mat} with its more intuitive graph adjacency representation, it is preferable to use Gemini-2.5 Pro over GPT-4o.
- 4) Analysis of the frequency gaps among the TRFs reveals that the preferences in Conn and Cyc are more pronounced, with larger variations in frequency. This is followed by BGM, and then TS, SP, MF, and HP, where the frequency gaps are more moderate.

D. D. Proof

We here provide the theorem with proof to demonstrate the pareto optimality of ideal dynamic routing.

Theorem 2 (GRE-based Dynamic Routing Pareto Optimality). *For any question distribution \mathcal{D}_q and tradeoff parameter $\alpha > 0$, the optimal router R^* satisfying $\forall f \in \mathcal{F}_{ZS}, R^* \succ R_f$, where R^* always select a TRF $f_q^{R^*} \in \mathcal{F}_q^*$, and R_f represents the routing always select f . The strict inequality establishes when f is suboptimal for any $q \in \text{supp}(\mathcal{D}_q)$.*

Proof. Given $E_f^k(q) = \text{Acc}_f^k(q) + \alpha \text{Eff}_f^k(q)$. For any fixed mode f :

$$\begin{aligned} \mathbb{E}_q[E_{f_q^{R^*}}^k(q)] &= \mathbb{E}_q \left[\max_{m' \in \mathcal{M}} E_{m'}^k(q) \right] \\ &\geq \mathbb{E}_q[E_f^k(q)] \quad (\text{pointwise optimality}) \\ &= \mathbb{E}_q[\text{Acc}_f^k(q)] + \alpha \mathbb{E}_q[\text{Eff}_f^k(q)] \end{aligned}$$

Model	TRFs	Conn	Cyc	TS	SP	MF	BGM	HP
GPT-4o	1st	V_{fdp} (92.3%)	V_{sfdp} (85.1%)	T_{set} (58.5%)	T_{set} (19.5%)	T_{list} (21.7%)	V_{dot} (34.2%)	T_{list} (30.4%)
	2nd	V_{neato} (92.1%)	V_{fdp} (12.9%)	T_{list} (36.2%)	V_{neato} (18.7%)	T_{set} (20.8%)	V_{circo} (20.3%)	T_{set} (20.3%)
	3rd	V_{sfdp} (91.7%)	V_{dot} (12.2%)	V_{dot} (23.1%)	T_{list} (17.1%)	T_{mat} (16.7%)	V_{neato} (19.8%)	V_{circo} (18.8%)
	4th	V_{circo} (84.4%)	V_{circo} (10.5%)	T_{mat} (0.8%)	V_{fdp} (16.3%)	V_{neato} (10.8%)	V_{sfdp} (13.4%)	V_{dot} (17.4%)
	5th	V_{dot} (73.0%)	V_{fdp} (61.1%)	V_{sfdp} (0.8%)	V_{circo} (13.8%)	V_{fdp} (8.3%)	V_{fdp} (9.1%)	V_{sfdp} (15.9%)
	6th	T_{list} (27.0%)	T_{list} (10.8%)	V_{neato} (0.8%)	V_{sfdp} (12.2%)	V_{dot} (7.5%)	T_{list} (7.0%)	V_{neato} (14.5%)
	7th	T_{mat} (58.0%)	T_{mat} (0.2%)	V_{circo} (0.8%)	V_{dot} (10.6%)	V_{circo} (7.5%)	T_{set} (1.6%)	T_{mat} (7.2%)
	8th	T_{set} (47.7%)	T_{set} (0.0%)	V_{fdp} (0.8%)	T_{mat} (6.5%)	V_{sfdp} (6.7%)	T_{mat} (0.5%)	V_{fdp} (0.0%)
Gemini 2.5 Pro	1st	V_{neato} (88.8%)	V_{neato} (97.2%)	T_{set} (41.0%)	T_{list} (48.6%)	T_{mat} (40.0%)	V_{fdp} (24.4%)	T_{list} (42.9%)
	2nd	V_{fdp} (88.2%)	V_{sfdp} (93.0%)	T_{list} (30.3%)	T_{mat} (37.6%)	T_{list} (36.0%)	V_{sfdp} (14.5%)	T_{set} (31.7%)
	3rd	V_{sfdp} (88.2%)	V_{dot} (71.8%)	T_{mat} (15.4%)	T_{set} (26.6%)	T_{set} (14.0%)	V_{neato} (14.5%)	T_{mat} (30.2%)
	4th	V_{circo} (87.0%)	V_{circo} (71.1%)	V_{dot} (6.9%)	V_{sfdp} (13.8%)	V_{sfdp} (6.0%)	V_{dot} (13.7%)	V_{fdp} (9.5%)
	5th	V_{dot} (83.4%)	V_{neato} (8.3%)	V_{fdp} (4.3%)	V_{dot} (11.0%)	V_{neato} (2.0%)	T_{mat} (12.2%)	V_{circo} (9.5%)
	6th	T_{list} (61.3%)	T_{list} (0.5%)	V_{neato} (2.1%)	V_{fdp} (8.3%)	V_{circo} (2.0%)	V_{circo} (9.2%)	V_{sfdp} (9.6%)
	7th	T_{mat} (8.5%)	T_{mat} (5.2%)	V_{sfdp} (0.0%)	V_{circo} (4.6%)	V_{dot} (0.0%)	T_{set} (6.9%)	V_{dot} (0.0%)
	8th	T_{set} (5.1%)	T_{set} (2.1%)	V_{fdp} (0.8%)	V_{neato} (2.8%)	V_{fdp} (0.0%)	T_{list} (5.3%)	V_{neato} (0.0%)

Table A11: Complete ranking of TRFs with respect to their label frequency in the TRFP dataset of GPT-4o and Gemini-2.5 Pro. By differing visual or textual TRFs with colors, **the special preference patterns of tasks are explicitly exposed**.

Rearranging terms, we have $\mathbb{E}_q[\text{Acc}_{f_q^{R^*}}^k(q)] - \mathbb{E}_q[\text{Acc}_f^k(q)] \geq \alpha \left(\mathbb{E}_q[\text{Eff}_f^k(q)] - \mathbb{E}_q[\text{Eff}_{f_q^{R^*}}^k(q)] \right)$. If $\mathbb{E}_q[\text{Eff}_{f_q^{R^*}}^k(q)] < \mathbb{E}_q[\text{Eff}_f^k(q)]$, the RHS becomes positive, forcing $\mathbb{E}_q[\text{Acc}_{f_q^{R^*}}^k(q)] > \mathbb{E}_q[\text{Acc}_f^k(q)]$. Otherwise $\mathbb{E}_q[\text{Eff}_{f_q^{R^*}}^k(q)] \geq \mathbb{E}_q[\text{Eff}_f^k(q)]$ directly holds. Thus R^* either strictly improves accuracy while matching efficiency, or maintains accuracy while strictly improving efficiency. This establishes Pareto dominance over any fixed mode m . \square

E E. Data and Task Details

E.1 Task Introduction

We introduce Tasks in this section. The 7 in-domain graph algorithmic QA tasks include:

- **Connectivity** (Sedgewick 2001) (abbreviated as Conn): Assess whether two randomly chosen nodes u and v in an undirected graph are linked.
- **Cycle** (Sedgewick 2001) (abbreviated as Cyc): Determine if there is a cycle present within an undirected graph.
- **Topological Sort** (Kahn 1962) (abbreviated as TS): Identify a valid topological ordering for a directed acyclic graph. This sort provides a sequence of nodes such that for every directed edge $u \leftarrow v$, node u precedes node v in the sequence.
- **Shortest Path** (Dijkstra 1959) (abbreviated as SP): Locate the shortest route between two nodes in a weighted undirected graph. The shortest path is defined as the route with the smallest total edge weight connecting the two nodes.
- **Maximum Flow** (Ford and Fulkerson 1956) (abbreviated as MF): Compute the maximum flow from a source node to a destination node in a network graph.
- **Bipartite Graph Matching** (Karp, Vazirani, and Vazirani 1990) (abbreviated as BGM): Identify the largest matching set in a bipartite graph. A matching set consists of edges where no two edges share a common node.
- **Hamilton Path** (Gould 2003) (abbreviated as HP): Discover a Hamiltonian path in an undirected graph. This path visits each node exactly once.

The 2 out-of-domain downstream application tasks are:

- **Link Prediction**: Predict whether a link or edge exists between two nodes in a network, based on the current structure and attributes of the graph. It is one of the cornerstone tasks in graph learning and has wide applications in social network analysis (Cao et al. 2020), recommendation systems (He et al. 2020), and biological network studies (Yamanishi et al. 2008).
- **Node Classification**: This task is concerned with predicting the categories of nodes within a graph. Node classification is widely used in applications such as community detection (Newman and Girvan 2004), fraud detection (Akoglu, Tong, and Koutra 2015), and identifying roles in social networks (Wasserman and Faust 1994).

E.2 Dataset Statistics

We adopt the GVLQA-BASE (Wei et al. 2024b) benchmark for in-domain tasks. For out-of-domain applications, we adopt the ca-GrQC and ca-HepTh (Leskovec, Kleinberg, and Faloutsos 2007) datasets for link prediction (LP), and use the PolBlog (Adamic and Glance 2005) and Cora (Yang, Cohen, and Salakhudinov 2016) datasets for the node classification (NC) task. Data statistics are provided in Table A12 and A13.

	Conn	Cyc	TS	SP	MF	BGM	HP
#sample	16,410	4,100	2,910	1,560	1,500	1,860	900
#nodes	25.01	23.42	21.86	13.65	13.90	21.13	13.24
#edges	95.46	23.66	114.10	23.99	49.16	51.03	45.05

Table A12: Data Statistics for in-domain graph algorithmic QA tasks.

	ca-GrQC	ca-HepTh	PolBlogs	Cora	CiteSeer
# Nodes	5,242	9,877	1,490	2,708	3,327
# Edges	14,496	25,998	19,025	5,278	4,676
domain	collaboration	collaboration	social	citation	citation
average degree	5.53	5.26	25.54	3.9	2.74

Table A13: Data Statistics for downstream applications

F E. Implementation Details

In our experiment, we use DeBERTaV3-base as TRF Router, which is trained with learning rate $\in \{5e-5, 5e-6\}$, weight decay $\in \{1e-2, 1e-3\}$, epoch $\in \{6, 8, 10\}$, batch size $\in \{16, 32, 64\}$. All experiments are conducted on a single NVIDIA A100 GPU. For all methods in comparison, the task instructions are unified in Table A14, which is followed by a control instruction (provided in A15) to specify the place and format of the answer to be extracted. More implementation details for each method are as follows:

- GPT-4o/Gemini-2.5 Pro: For the backbone LMMs, we examine their graph QA performances by invoking the official API Interface to directly answer the questions with instructions. Due to the prevalent nature of edge set in existing works, we adopt T_{set} to represent the graph topology during implementation.
- Vanilla Chain-of-thought (CoT) (Wei et al. 2022): CoT has demonstrated that the simple prompts that drive the LMMs in analytical, step-by-step thinking can boost the general range of capabilities of LMM reasoning. We adopt CoT in our baseline by appending a sentence of CoT prompt in the input tail: “Please think step by step and present the rationales in a well-structured manner, to make the answer more reliable and robust.”. Due to the prevalent nature of edge set in existing works, we adopt T_{set} to represent the graph topology during implementation.
- NLGraph (Wang et al. 2023)/ GraphDPR (Li et al. 2024)/ GITA (Wei et al. 2024b): NLGraph proposes to use BAG prompting to conceptualize a graph and algorithmic prompting to specify the algorithm. GraphDPR proposes to employ the external graph algorithmic toolkits to generate intermediate descriptions and code, which are utilized to enhance multi-step reasoning. GITA simultaneously adopts a visual TRF and (similar to V_{dot}) a textual TRF (Similar to T_{set}) to solve graph algorithmic problems by leveraging the complementary nature of the visual and textual mutual-enhancement across tasks. We evaluate these methods based on their own official implementations, but modifying the prompt templates to that we have specified in Table A8, A14, and A15.

G G. TRF Router versus single TRFs (both GPT-4o and Gemini-2.5 Pro)

To demonstrate the importance of the proposed TRF Routing, we present metrics comparing individual TRFs with the TRF Router within the DynamicTRF framework. Additionally, we include the performance of ‘*Ideal Routing*’, where the TRF with the optimal Global Routing Efficiency (GRE) is always selected, representing the upper bound capability of TRF routing.

While we have already presented such analysis for GPT-4o in our manuscript in section 5.3 based on Table 5, it is important to note that Table 5 only contains results for GPT-4o. Here, we provide a complete comparison table including the results for Gemini-2.5 Pro in Table A16. The observations for Gemini-2.5 Pro are similar to those we have reported in section 5.3 for GPT-4o, indicating that there is no single dominant TRF across all tasks. The top TRFs for each task align closely with the task preferences shown in the TRFP dataset (Table A11).

Tasks	Task Instruction
Connectivity	Is there a path between node [P] and node [P] in this undirected graph?
Cycle	Is there a cycle in this undirected graph?
Topological Sort	This representation depicts a directed graph, in which each directed edge from node A to node B signifies that, according to the topological order, node A must precede node B. Q: The topological order of the directed graph is:
Shortest Path	This representation illustrates a directed graph, with each edge's capacity indicated by a numerical label in close proximity. Q: What is the maximum flow from node 4 to node 0:
Maximum Flow	This representation illustrates a directed graph, with each edge's capacity indicated by a numerical label in close proximity. Q: What is the maximum flow from node [P] to node [P]:
Bipartite Graph Matching	There are [P] hosts numbered from [P] to [P], and [P] tasks numbered from [P] to [P]. Each host has a set of tasks that it is interested in, represented by arrows from a host to a task in the diagram. However, each host is capable of solving only one task, and similarly, each task can be resolved by just one host. Q: What is the maximum number of hosts that can be assigned a task they are interested in?
Hamilton Path	Q: Begin with node 0, what is the path in this graph that visits every node exactly once?
Link Predict	The task is link prediction, aiming to predict the presence or absence of an unknown edge between Node [P] and Node [P] based on the known graph structure. Q: Does an unknown edge exist between Node [P] and Node [P]?
Node Classify	The task is semi-supervised node classification, and needs to predict which class Node [P] belongs to, based on graph structure and known node classes. Q: Node [P] belongs to Class: Note that capacity is directional, allowing flow only in the edge direction; reverse edge direction should not be considered in the path.

Table A14: Unified Task Instructions in experimental comparisons, where [P]s are placeholders that will be substituted in specific questions.

Tasks	Task Instruction
Connectivity/ Cycle/ Link Predict	Please put the answer between <answer> and </answer> tags. For example, <answer>Yes</answer> or <answer>No</answer>.
Topological Sort/ Shortest Path/ Hamilton Path	Please put the answer between <answer> and </answer> tags. For example, <answer>0->1->2->3->4</answer> or <answer>0->1->3->7->8->4->6->5->9->2</answer>.
Maximum Flow	Please put the answer between <answer> and </answer> tags. For example, <answer>3</answer> or <answer>8</answer>.
Node Classify	Please put the answer between <answer> and </answer> tags. For example, <answer>Class 1</answer> or <answer>Class 3</answer>.

Table A15: Control Task Instructions in experimental comparisons.

With the TRF Router, DynamicTRF achieves the highest GRE scores across all tasks compared to individual TRFs, showcasing its superior performance in balancing accuracy and efficiency. However, there still exists a gap between the TRF Router and ‘Ideal Routing’, emphasizing the continued potential of TRF routing.

TRF	Conn		Cyc		TS		SP		MF		BGM		HP	
	Acc(Tok)	GRE	Acc(Tok)	GRE	Acc(Tok)	GRE	Acc(Tok)	GRE	Acc(Tok)	GRE	Acc(Tok)	GRE	Acc(Tok)	GRE
<i>GPT-4o</i>														
V_{dot}	78.5(8.4)	27.1	80.0(8.0)	28.3	12.3(346.0)	0.7	14.5(146.3)	1.2	7.5(410.2)	0.4	<u>91.2(244.3)</u>	<u>5.8</u>	13.3(40.0)	2.1
V_{neato}	95.1(7.7)	34.3	87.1(8.0)	30.8	3.0(30.0)	0.5	20.0(130.1)	1.8	10.8(387.4)	0.5	87.2(280.0)	5.2	11.1(40.0)	1.8
V_{circo}	89.7(8.2)	31.3	70.7(8.0)	25.0	3.0(30.0)	0.5	18.2(153.5)	1.5	8.1(421.3)	0.4	88.2(271.6)	5.3	14.4(40.0)	2.3
V_{fdp}	<u>96.0(8.1)</u>	<u>33.6</u>	60.5(8.0)	21.4	3.0(30.0)	0.5	17.3(150.5)	1.4	8.1(389.2)	0.4	82.9(295.3)	4.8	4.4(74.0)	0.5
V_{sfdp}	94.8(8.1)	33.3	85.1(7.0)	32.2	7.0(120.0)	0.6	25.5(168.7)	2.0	8.1(386.1)	0.4	84.0(302.9)	4.8	12.2(40.0)	1.9
T_{set}	92.5(273.3)	5.6	52.7(480.6)	2.4	<u>36.6(224.2)</u>	<u>2.4</u>	54.6(566.0)	2.3	<u>25.3(362.9)</u>	<u>1.3</u>	69.5(370.1)	3.6	<u>50.0(124.9)</u>	4.5
T_{list}	89.0(218.2)	6.0	53.2(359.7)	2.8	34.2(206.3)	2.4	<u>55.5(518.9)</u>	<u>2.4</u>	24.2(400.7)	1.2	65.8(410.8)	3.2	50.0(107.0)	<u>4.8</u>
T_{mat}	79.9(233.7)	5.2	52.7(417.1)	2.6	6.8(378.1)	0.4	34.5(591.8)	1.4	17.2(402.9)	0.9	60.4(407.3)	3.0	31.1(160.9)	2.5
TRF Router	96.1(38.8)	15.4	89.3(75.9)	10.3	41.4(176.1)	3.1	68.4(499.1)	3.1	36.6(385.2)	1.9	92.0(233.6)	6.0	61.1(76.3)	7.0
Ideal Routing	100(7.9)	35.6	100(7.1)	37.6	44.5(268.0)	2.7	81.8(223.4)	5.5	53.8(380.0)	2.8	100(181.7)	7.4	76.7(72.2)	9.0
<i>Gemini-2.5 Pro</i>														
V_{dot}	94.1(8.4)	32.5	72.5(8.0)	25.6	23.2(1157.0)	0.7	46.8(846.0)	1.6	14.6(1113.5)	0.4	93.9(1023.7)	2.9	30.6(1196.0)	0.9
V_{neato}	99.6(7.7)	35.8	97.9(8.0)	34.6	7.9(885.0)	0.3	53.2(866.9)	1.8	25.0(1173.3)	0.7	96.5(1005.7)	3.0	27.4(1056.0)	0.8
V_{circo}	98.4(9.5)	31.9	71.1(8.0)	25.1	3.0(1106.0)	0.1	40.4(852.8)	1.4	8.3(1056.4)	0.3	91.3(1137.7)	2.7	226.0(30.0)	<u>4.1</u>
V_{fdp}	<u>99.6(997.0)</u>	32.0	61.0(8.0)	21.6	6.1(638.0)	0.2	44.0(856.8)	1.5	18.8(1158.0)	0.6	<u>98.3(948.2)</u>	<u>3.2</u>	21.0(30.0)	3.8
V_{sfdp}	99.4(8.4)	<u>34.4</u>	93.7(8.0)	<u>33.1</u>	5.5(1585.0)	0.1	46.8(828.7)	1.6	16.7(1178.7)	0.5	95.7(1042.2)	3.0	30.6(891.0)	1.0
T_{set}	97.2(218.7)	6.6	<u>98.6(716.6)</u>	3.7	84.1(1395.9)	<u>2.3</u>	93.6(810.8)	3.3	91.7(1154.9)	2.7	97.1(1076.8)	3.0	96.8(678.1)	3.7
T_{list}	97.4(155.3)	7.8	96.5(652.8)	3.8	76.8(1532.3)	2.0	96.3(601.0)	3.9	92.2(1035.8)	2.9	97.6(1129.9)	2.9	97.0(646.1)	3.8
T_{mat}	97.6(176.1)	7.4	96.5(720.8)	3.6	68.9(1554.7)	1.7	93.6(728.7)	<u>3.5</u>	95.8(1042.6)	<u>3.0</u>	96.9(1033.8)	3.0	<u>98.4(737.0)</u>	3.6
TRF Router	100(12.9)	27.8	99.3(16.7)	24.3	87.8(1191.2)	2.5	96.3(798.6)	3.4	100(1004.8)	3.2	100(776.0)	3.6	100(254.6)	6.3
Ideal Routing	100(7.9)	35.6	100(7.1)	37.6	44.5(268.0)	2.7	81.8(223.4)	5.5	53.8(380.0)	2.8	100(181.7)	7.4	76.7(72.2)	9.0

Table A16: Comparison of the DynamicTRF framework with TRF Router versus single TRFs on in-domain tasks. ‘Ideal Routing’ means the routing is always to the best TRF.